INDC(NDS)-0711, Rev. 1
Distr. AC

IAEA
International Atomic Energy Agency

INDC International Nuclear Data Committee

URR-PACK: Calculating Self-Shielding in the Unresolved Resonance Energy Range

Dermott E. Cullen
1466 Hudson Way, Livermore, CA 94550, U.S.A.

Andrej Trkov
International Atomic Energy Agency, Vienna, Austria

July 2016

IAEA Nuclear Data Section
Vienna International Centre, P.O. Box 100, 1400 Vienna, Austria

Selected INDC documents may be downloaded in electronic form from
http://www-nds.iaea.org/publications
or sent as an e-mail attachment.
Requests for hardcopy or e-mail transmittal should be directed to
NDS.Contact-Point@iaea.org
or to:
Nuclear Data Section
International Atomic Energy Agency
Vienna International Centre
PO Box 100
1400 Vienna
Austria

Printed by the IAEA in Austria

July 2016

INDC(NDS)-0711, Rev. 1
Distr. AC

URR-PACK: Calculating Self-Shielding in the Unresolved Resonance Energy Range

Dermott E. Cullen
1466 Hudson Way, Livermore, CA 94550, U.S.A.

Andrej Trkov
International Atomic Energy Agency, Vienna, Austria

July 2016

Contents

Overview

Revision 1 of this report (July 2016) describes the 2016-2 version of the URRDO and URFIT computer codes. Most of the difference in this document between the original and revision 1 is in the Appendix describing how to analytically define multi-band parameters. There is a typo in ref. [6], [7], and the original version of this report. In calculating multi-band parameters the correct definition of B^2 is,

$$B^2 = \{ < \Sigma_1 > A [< \Sigma_0 > A - 2] + 1 \} / [< \Sigma_0 >< \Sigma_1 >]$$

This only effects the documentation; the codes GROUPIE [10], URRDO and URRFIT have always used the correct definition of B^2.

This report describes HOW to calculate self-shielding in the unresolved resonance region (URR) [1], in terms of the computer codes we provide to allow a user to do these calculations himself. Here we only describe HOW to calculate; a longer companion report describes in detail WHY it is necessary to include URR self-shielding.

Presently NJOY [2] uses the Probability Table Method (PTM) [3] to define self-shielding factors for subsequent use by MCNP [4]; this PTM data uses 20 cross section bands. Here we provide the computer tools needed to replace these 20 band data by Multi-band [5, 6, 7] (MB) data using only 2 cross section bands, and we demonstrate that this 2 band MB data produce statistically identical macroscopic K-eff results to those obtained by MCNP using 20 bands with the probability table method (PTM).

The format for the representation of PTM and MB data is identical, so that we were able to easily interchange them and run MCNP with ABSOLUTELY NO CHANGES to MCNP – PTM and MB are 100% compatible and MCNP had no idea whether it was using one or the other – the only difference being 20 bands for PTM and only 2 bands for MB.

The method described here to define self-shielded cross sections in the unresolved resonance region (UUR) by extrapolating moments of the cross section from the resolved to unresolved resonance region, is not new; it has been used in the TART Monte Carlo code since circa 1975 [5, 6, 7]. I (D.E. Cullen) never bothered to publish the method because it always seemed so obvious to me, that I assumed it was widely known. In fact since I implemented it in TART I have not seen it used in any other code, so I am documenting it here, but I am stressing that it is by no means new or original.

The tasks we wish to cover here include,

1) Demonstrate that URR self-shielding is needed to accurate calculate results.
2) Demonstrate that the multi-band method (MB) [5, 6, 7], using only 2 cross section bands, gets statistically the same answers as the Probability Table Method (PTM) [3] using 20 bands; here we use the NJOY-generated 20 band PTM data to generate the 2 band MB data.
3) Demonstrate that the method which D.E. Cullen has used for decades to define Multi-band Parameters for use with the TART Monte Carlo code [9], also produces essentially the same answers as MCNP using 20 bands. Unlike step 2) described

above, here we derive the MB parameters completely independently of the method used by NJOY.

To accomplish these tasks we provide URR-PACK, which is composed of three computer codes,

1) GROUPIE – A standard code from PREPRO [10]. We use this to calculate self-shielding factors and multi-band (MB) parameters over the entire energy range; not just the unresolved resonance region. The GROUPIE (Version 2016) code now prints out information that we need to run the URRFIT code described below.

```
Resolved Resonance Region..... 1.00000E-5 to  600.000000 eV
Complete Input Parameters for URRFIT are listed below
ZA.............................      92233
MAT............................       9222
Atomic Weight Ratio (ATWT).... 231.037700
Unresolved Resonance Region... 600.000000 to  40000.0000 eV
Unresolved Competition (ICOMP)           0
Is Unresolved Tabulated (LSSF)           1
```

2) URRDO – Start from the present standard NJOY/MCNP Probability Table Method (PTM) data, in a pseudo-ENDF format, and transform these data to other forms for use in our testing at described below, including: no self-shielding, and self-shielding using Multi-band (MB), rather than PTM, parameters.

3) URRFIT - Start from GROUPIE output of Multi-band (MB) parameters over the entire energy range, except for the unresolved resonance region. Use this to create self-shielding factors in the unresolved resonance region. Output is provided in several formats that can be used by MCNP [3] and TART [9]. The input data required are exactly those output by GROUPIE, described above,

```
92233       9222   231.0377    600.0     40000.0          0    1
u233.multband
u233.multband.new
U233.URRFIT.NJOY
------------(Nothing below this line is Read)-------------------------
   ZA         MAT   At.Wt.      E-Low     E-High        ICOMP LSSF
```

The difference between the NJOY/MCNP results produced by URRDO and URRFIT, is that the URRDO Multi-band (MB) parameters are produced starting from PTM parameters generated by NJOY, so this relies on the NJOY code to produce the basic data. The URRFIT results are completely independent of NJOY, and only rely on GROUPIE and the method that has been used for decades to produce Multi-band (MB) data for use with the TART code.

A Brief History of the Unresolved Resonance Region

When Leo Levitt first developed his Probability Table Method (PTM) circa 1970 [3], the unresolved resonance region was more important than it is today, because it spanned a larger energy range. As the years have passed the resolved resonance region has been extended to higher and higher energies, resulting in smaller unresolved resonance regions, thereby reducing its importance and simplifying our treatment. We can easily see this by comparing the current ENDF/B-VII.1 data to the earlier, circa 1970, ENDF/B-II data.

For ^{235}U ENDF/B-II the resolved resonance region was 1 eV to 64.504 eV, and the unresolved 64.504 eV to 24,788 eV; in comparison for ^{235}U ENDF/B-VII.1 the resolved region is 10^{-5} eV to 2,250 eV, and the unresolved 2,250 eV to 25,000 eV. Here the upper energy limit of the unresolved region is essentially the same, but the lower energy limit has increased from 64.504 eV to 2,250 eV, greatly shortening the unresolved resonance region.

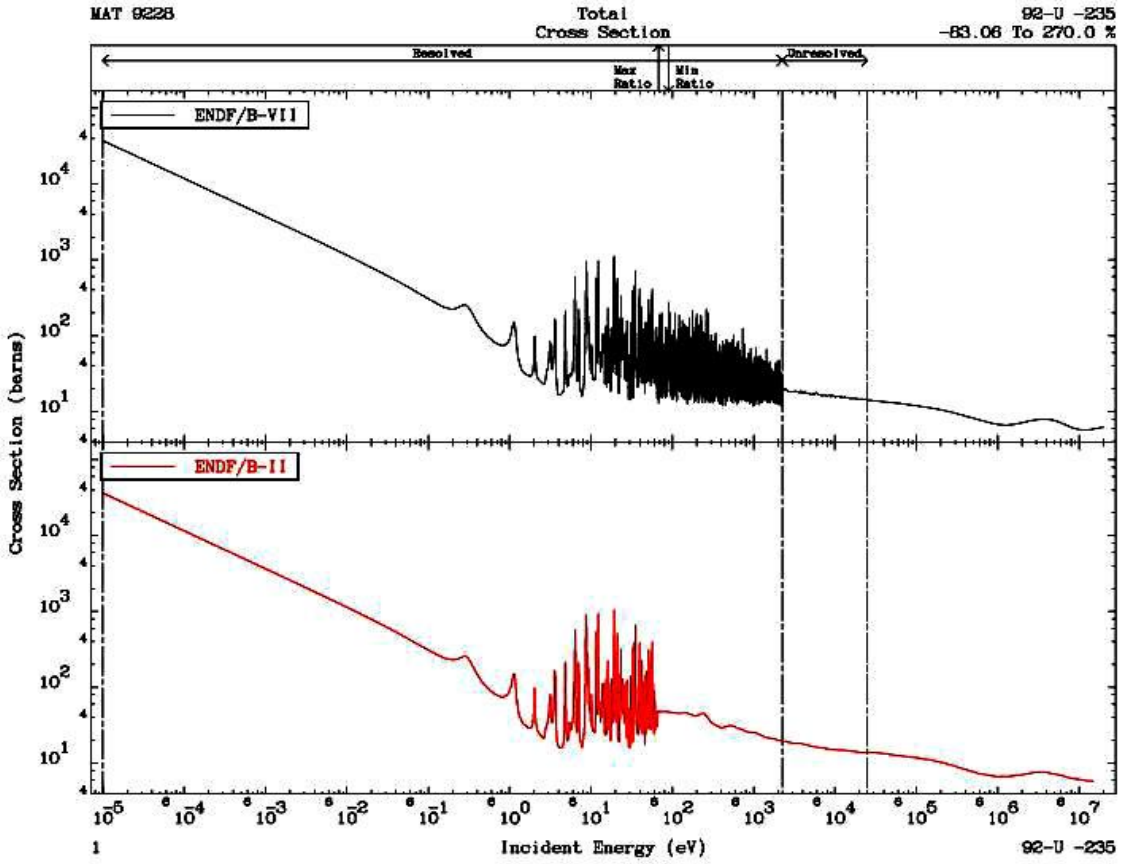

Fig. 1: *Total cross section of ^{235}U from the ENDF/B-VII.1 and the ENDF/B-II libraries.*

For ^{238}U ENDF/B-II the resolved resonance region was 5 eV to 3,910 eV, and the unresolved 3,910 eV to 45,000 eV; in comparison to ^{238}U ENDF/B-VII.1 the resolved region is 10^{-5} eV to 20,000 eV, and the unresolved 20,000 eV to 149,028 eV. Here the upper energy limit of the unresolved region has been increased, but the lower energy limit has increased from 3,910 eV to 20,000 eV, greatly shortening the unresolved resonance region.

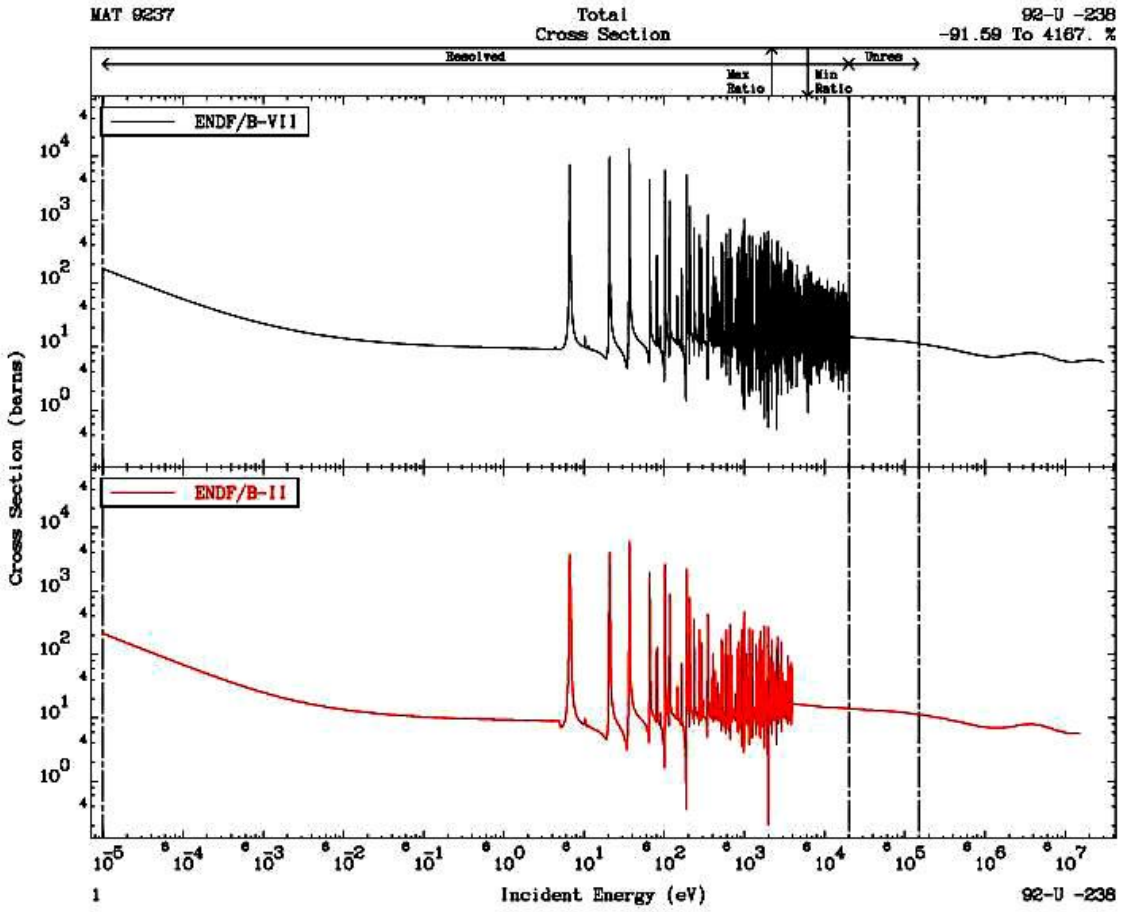

Fig. 2: *Total cross section of ^{238}U from the ENDF/B-VII.1 and the ENDF/B-II libraries.*

Compared to the problem that Leo Levitt faced and solved circa 1970, today as a result of these changes in evaluations it is actually easier for us to extrapolate important moments of the cross section from the resolved to unresolved regions; we have more information about the larger resolved regions and less of an energy range to extrapolate to in order to span the unresolved regions.

URRDO Code

The first 2 steps described above are addressed by the URRDO code. This code starts from the NJOY unresolved resonance region self-shielding data in a pseudo-ENDF format (i.e., an unofficial format created and used solely by NJOY). Based on reading this NJOY output data URRDO will produce one of three types of output,

1) Identical to the Original NJOY data, allows us to "see" and check NJOY PTM data,
2) Similar to the Original Data but with Self-Shielding Turned off.
3) The Original 20 band PTM data replaced by 2 band MB Data.

Using the Original NJOY data and the above described URRDO output we were able to perform MCNP runs of three different types using a collection of 32 critical assemblies and comparing the K-eff calculated results. Below is a table of the 32 critical assemblies used here for testing (the index numbers 1 through 32 will be used to refer to the different cases).

No.	ICSBEP label	Short name	Common name
1	HEU-MET-FAST-001	hmf001	Godiva
2	HEU-MET-FAST-002	hmf002-2	Topsy-2
3	HEU-MET-FAST-003	hmf003-01	Topsy-U_2.0in(Uranium reflector)
4	HEU-MET-FAST-003	hmf003-02	Topsy-U_3.0in(Uranium reflector)
5	HEU-MET-FAST-003	hmf003-03	Topsy-U_4.0in(Uranium reflector)
6	HEU-MET-FAST-003	hmf003-10	Topsy-W_4.5in(Tungsten reflector)
7	HEU-MET-FAST-003	hmf003-11	Topsy-W_6.5in(Tungsten reflector)
8	HEU-MET-FAST-014	hmf014	VNIIEF-CTF-DU
9	HEU-MET-FAST-032	hmf032-1	COMET-TU1_3.93in
10	HEU-MET-FAST-032	hmf032-2	COMET-TU1_3.52in
11	HEU-MET-FAST-032	hmf032-3	COMET-TU1_1.742in
12	HEU-MET-FAST-032	hmf032-4	COMET-TU1-0.683in
13	IEU-MET-FAST-007	imf007	Big_Ten
14	IEU-MET-FAST-007	imf007d	Big_Ten(detailed)
15	IEU-MET-FAST-010	imf010	ZPR-6/9(U9)
16	IEU-MET-FAST-013	imf013	ZPR-9/1(Tungsten reflector)
17	IEU-MET-FAST-014	imf014-2	ZPR-9/2(Tungsten reflector)
18	MIX-MISC-FAST-001	mif001-01	BFS-35-1
19	MIX-MISC-FAST-001	mif001-02	BFS-35-2
20	MIX-MISC-FAST-001	mif001-03	BFS-35-3
21	MIX-MISC-FAST-001	mif001-09	BFS-31-4
22	MIX-MISC-FAST-001	mif001-10	BFS-31-5
23	MIX-MISC-FAST-001	mif001-11	BFS-42
24	IEU-MET-FAST-022	imf022-01	FR0_3X-S
25	IEU-MET-FAST-022	imf022-02	FR0_5-S
26	IEU-MET-FAST-022	imf022-03	FR0_6A-S
27	IEU-MET-FAST-022	imf022-04	FR0_7-S
28	IEU-MET-FAST-022	imf022-05	FR0_8-S
29	IEU-MET-FAST-022	imf022-06	FR0_9-S
30	IEU-MET-FAST-022	imf022-07	FR0_10-S
31	IEU-MET-FAST-012	imf012	ZPR-3/41
32	IEU-COMP-FAST-004	icf004	ZPR-3/12

The test cases included in the analysis were selected from the ICSBEP Handbook [8] according to the following criteria:

- Benchmarks that are sensitive to the capture and fission of the two uranium isotopes in the epithermal energy region; the search for such benchmarks was done with the DICE package, that is available with ICSBEP (version 2014).
- Benchmarks that are sensitive to capture in ^{238}U in the energy region from 10 keV to 20 keV (the list was provided by O. Cabellos, OECD/NEA Data Bank).
- Availability of inputs for MCNP.
- Godiva benchmark was added because it is the most widely used benchmark.

Results:

All calculations with MCNP were done with identical inputs. The number of source particles was sufficient to reach uncertainties below 8 pcm (parts per 100 000). A few selected cases were re-run with an increased number of particles to pin-down statistically significant differences. We like to think/hope that today our Monte Carlo codes [4, 9] can reproduce K-eff for critical assemblies to within +/- 0.1% (100 pcm). What the results show are:

1) Calculations using MCNP with and without URR self-shielding result in differences in K-eff of over 1%, which is 10 times, (i.e. 1000%) the 0.1% accuracy we think we can achieve. These results prove that it is important to include URR Self-Shielding in order to achieve accurate results.

2) Comparison of MCNP results using 20 band PTM data and 2 band MB differ in all cases by 0.02% or less, and in most cases by less than 0.01%; i.e., an order of magnitude closer than the uncertainty we hope to achieve and consider significant. These results prove that using either the original 20 band PTM data or 2 band MB data derived from the PTM data, the calculated K-eff values using PTM and MB parameters resulting are indistinguishable for all practical purposes; they are an order of magnitude closer than the 0.1% we hope to achieve, producing differences near only 0.01%.

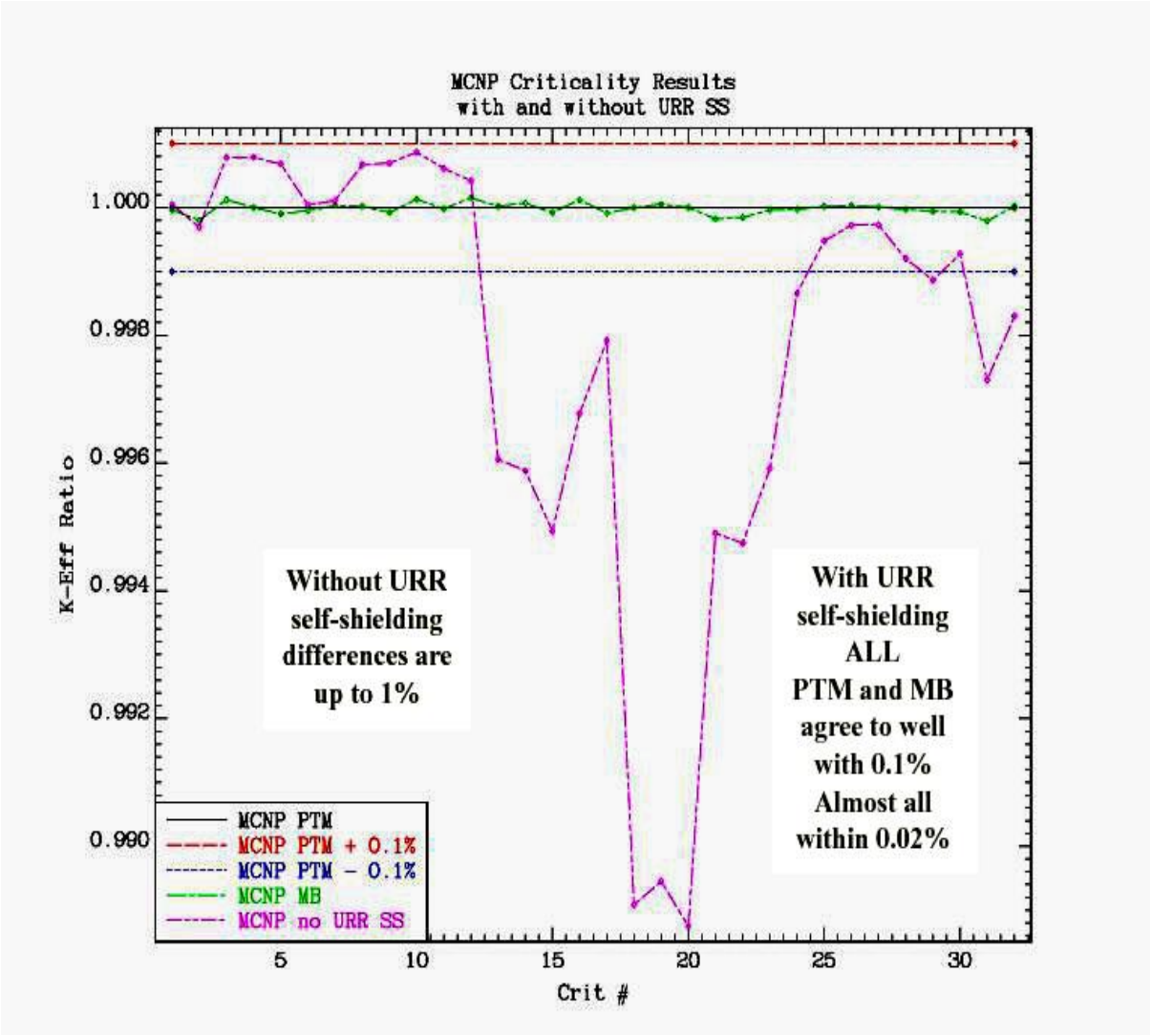

***Fig. 3**: Comparison of calculated K-eff values with and without self-shielding using PTM and MB parameters.*

URRFIT Code

The last (third) step described above is addressed by the URRFIT code. This code starts from GROUPIE Multi-band Parameters (MB) that are calculated from tabulated cross sections over the entire energy range; this tabulated data only include infinitely dilute cross sections in the unresolved resonance region. URRFIT adds self-shielding f-factors for the unresolved resonance region. This is completely independent of the method used by NJOY to calculate 20 band Probability Table Method (PTM) data.

The method used by URRFIT is not at all new; it has been used for decades to produce self-shielded data for use in the TART [9] Monte Carlo code. Over the decades many comparisons of the results with other codes were performed and published to demonstrate that this method produces accurate results. But this is the first time the author (D.E. Cullen) has shared the details of the method with the public; this is not to keep any important secret, rather it is because it was always felt that this method is so simple and obvious that surely many more people must have thought of it and used it before; but perhaps not, so the explanation follows below.

Let's talk Physics

For use in our applications we need a continuous and physically acceptable representation of our cross section over the entire range of neutron energies. In our evaluated neutron data we use a variety of representations for our cross sections in adjacent energy range. Generally we have a resolved resonance region at lower energies, followed by an unresolved resonance region, and at still higher energies we have smoothly varying tabulated data. Part of our job in preparing data for use in our applications is to combine these various representations to define a unique and physically acceptable continuous neutron cross sections over the entire neutron energy range.

To illustrate this point the below figure compares the ^{238}U Total cross section at temperatures of 0 and 300 K. In this figure we have: a resolved region up to 20 keV, an unresolved region from 20 to near 150 keV, and a tabulated smooth range above 150 keV. In this figure the unresolved resonance region is represented only by AVERAGE cross sections. In our neutron transport calculations we include the actual statistical fluctuations in the cross section within the unresolved region range; without including an unresolved region we would have a ridiculous non-physical representation of the cross section, as varying over orders of magnitude in the resolved region, and then abruptly becoming smooth at the resolved-unresolved energy boundary (in the below figure at 20 keV) and higher energies. By including an unresolved resonance region from 20 to near 150 keV we add a smooth transition between the resolved region below and the "smooth" tabulated data at higher energies that starts near 150 keV and extends upward from there. Again, let us stress that this is the whole purpose of the unresolved resonance region: allow a smooth and physically acceptable transition between resonance fluctuations and smooth tabulated cross sections.

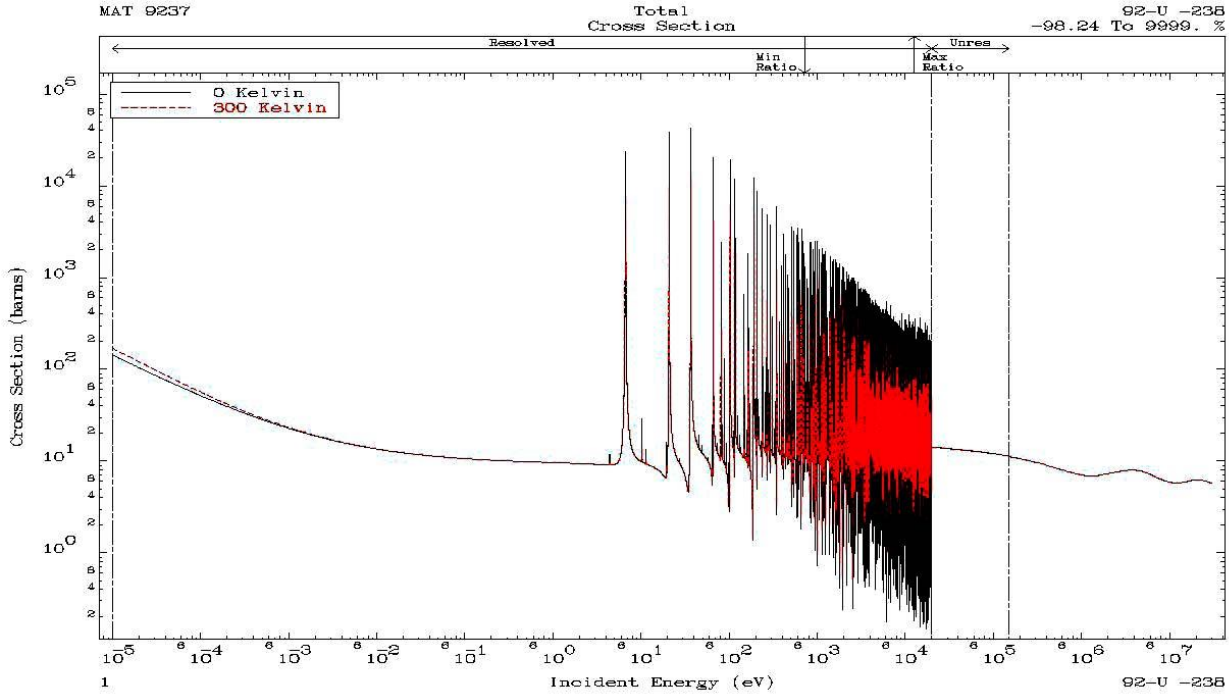

Fig. 4: *Total cross section of ^{238}U from the ENDF/B-VII.1 library at different temperatures.*

In our neutron transport calculations we are generally not interested in what happens at discrete energies; rather we are interested in integral observable properties, such as energy deposit, damage, etc. To be physically acceptable integral properties must be smoothly varying with energy, and in particular we expect them to smoothly vary across the artificial energy boundaries, between the resolved region at lower energy, followed by unresolved and finally "smooth" tabulated at higher energies. Let us stress again: physically nothing changes at these artificial energy boundaries; they are merely convenient man-made energy points used in our evaluations, and historically the transition energies have changed with time as our knowledge of the data improves.

Good physics tell us that nothing should abruptly happen at the artificial energy boundaries; rather we MUST have smooth variation across these boundaries. Therefore the approach used by URRFIT to define unresolved region self-shielding is to guarantee that they vary smooth between the resolved and unresolved region, and in addition that they smoothly approach the higher energy "smooth" tabulated data.

Hopefully the below figures illustrate that this objective is being met by URRFIT. In this case the GROUPIE code was used to calculate multi-group cross sections using the TART 616 group structure (50 groups per energy decade from 10^{-5} eV up to 20 MeV). Self-shielding factors are calculated in the resolved energy range, and these are then extrapolated from the resolved into the unresolved region, including a physically acceptable shape such that the self-shielding decreases, i.e., factors F_1 and F_2 (see the definitions below) approach unity toward the upper energy boundary of the unresolved region. The result is smoothly and continuously varying self-shielding across the entire neutron energy range. Note that with this method the infinitely dilute unresolved cross sections (that we now generally agree on) are preserved, and only self-shielding factors, F_1 and F_2, are extrapolated. The definition of the f-factors for the Total cross section $F_1(T)$ and $F_2(T)$ are:

$F_1(T) = \frac{\sum_B S_B P_B /[S_B + T]}{\sum_B P_B /[S_B + T]}$: sum over bands, B	$T = \sum_0 / < \sum_T (\infty) >$ $S_B = \sum_{TB} / < \sum_T (\infty) >$
$F_2(T) = \frac{\sum_B S_B P_B /[S_B + T]^2}{\sum_B P_B /[S_B + T]^2}$:sum over bands, B	$F_1(0)$ and $F_2(0)$ are the moments that are extrapolated from Resolved to Unresolved

You can consider $F_1(0)$ to be the totally shielded cross section. Personally I like to think of it as defining the reciprocal of the distance to collision; in our Monte Carlo codes we do not sample cross section, but rather we sample distance to collision, e.g.,

$$X = - \log(\text{random}) / \sum_T (E)$$

Similarly when we use the narrow resonance and Bonderenko approximations to calculate self-shielded multi-group cross sections, we are also calculating reciprocal distance to collision to define our group constants.

The combination of the moments F_1 and F_2 conserve distance to collision and its variance.

Extrapolation

Nuclear theory predicts that the self-shielding will decrease with increasing energy as $1/E$, so that the unresolved resonance region can indeed serve as a transition between the resonance fluctuations in the resolved resonance region, and the "smooth" tabulated cross sections at higher energy.

For decades this prediction has been used in the TART code to estimate the energy dependence of F_1 and F_2 in order to extrapolate from the resolved resonance region into the unresolved resonance region, to have a smooth, continuous variation of physics across the artificial resolved/unresolved energy boundary, and approach the "smooth" tabulated cross sections at higher energy. Specifically, the energy dependence is assumed to be:

$$F_1(E) = 1 - A_1/E$$

$$F_2(E) = 1 - A_2/E$$

where A_1 and A_2 are the fitting coefficients. The same factors can also be calculated directly from the self-shielded cross sections based on the unresolved resonance parameters, such as calculated by NJOY. By examining the below figures one can see that although the methods used by NJOY and the extrapolation method are completely different, they both show a similar $1/E$ decrease in self-shielding and differ only in how the coefficients A_1 and A_2 are defined in the above equations. NJOY uses a randomly sampled ladder of resonances, and an approximate method of Doppler broadening. In the extrapolation method we merely fit $F_1(E)$ and $F_2(E)$ in the resolved resonance region to define A_1 and A_2, and extrapolate this into the unresolved resonance region.

^{235}U Comparison of Unresolved Resonance Region Self-Shielding Factors

The ^{235}U unresolved energy range is from 2.25 keV to 25 keV. There is good agreement between both F_1 and F_2 factors for Total and Elastic, but the NJOY Fission and Capture F_2 is generally lower than URRFIT, and lower even than the range of F_2 in the resolved energy range; this is particular true of the Capture which is well below the entire range of F_2 in the resolved energy range; physically there should be a smooth, continuous variation with energy from resolved to unresolved. URRFIT results show this, whereas NJOY results do not.

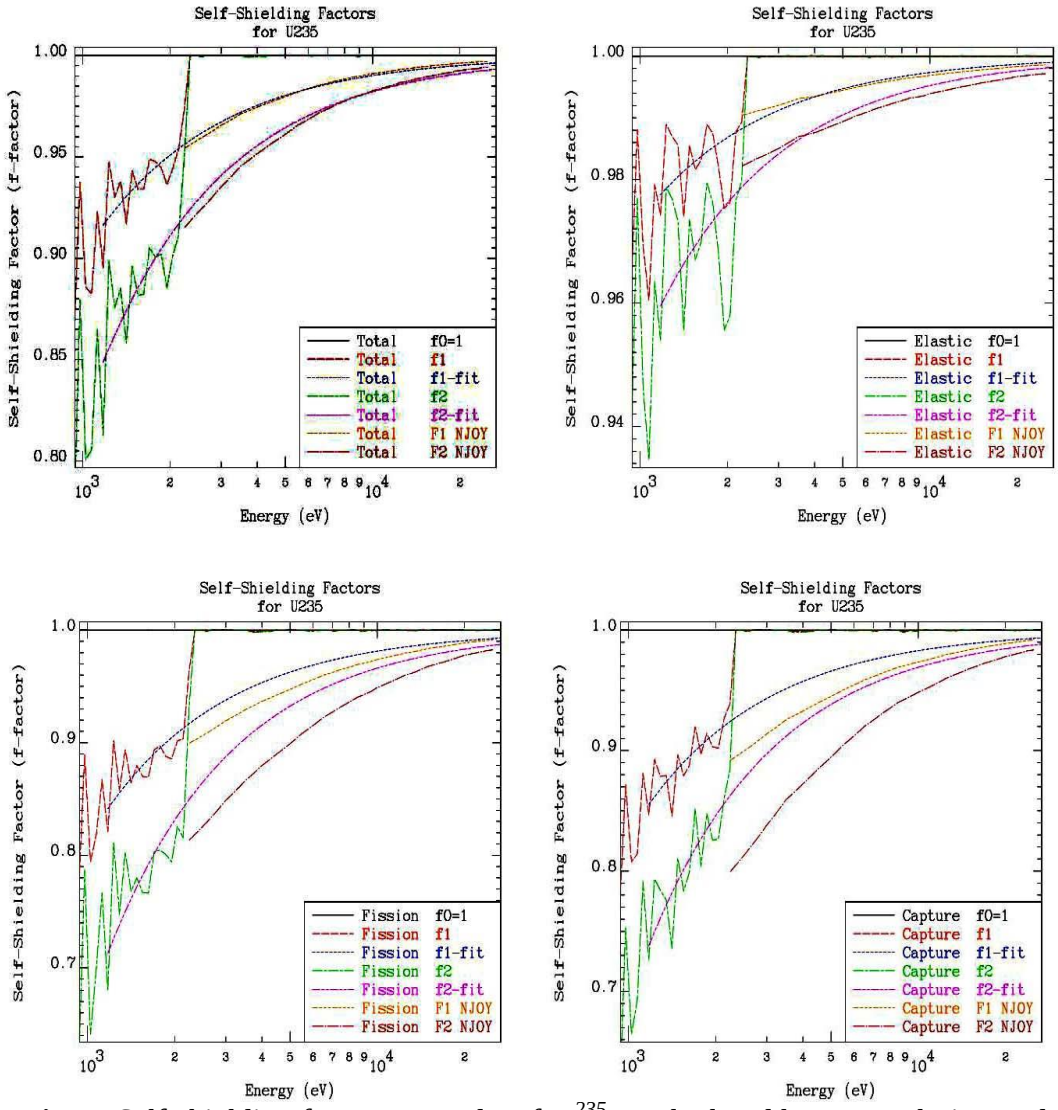

Fig. 5: *Self-shielding factors F_1 and F_2 for ^{235}U calculated by extrapolation and from the cross sections calculated by NJOY.*

^{238}U Comparison of Unresolved Resonance Region Self-Shielding Factors

The ^{238}U unresolved energy range is from 20 keV up to nearly 150 keV. Generally there is fair agreement in the F_1 factor calculated by URRFIT and NJOY, but the F_2 by NJOY is generally lower than the one by URRFIT, and it is even lower for Capture over the entire range of F_2 in the resolved range; physically there should be a smooth, continuous variation with energy from resolved to unresolved. URRFIT results show this, whereas NJOY results do not. Note, that NJOY has no data for fission, whereas the URRFIT results include the sub-threshold fission.

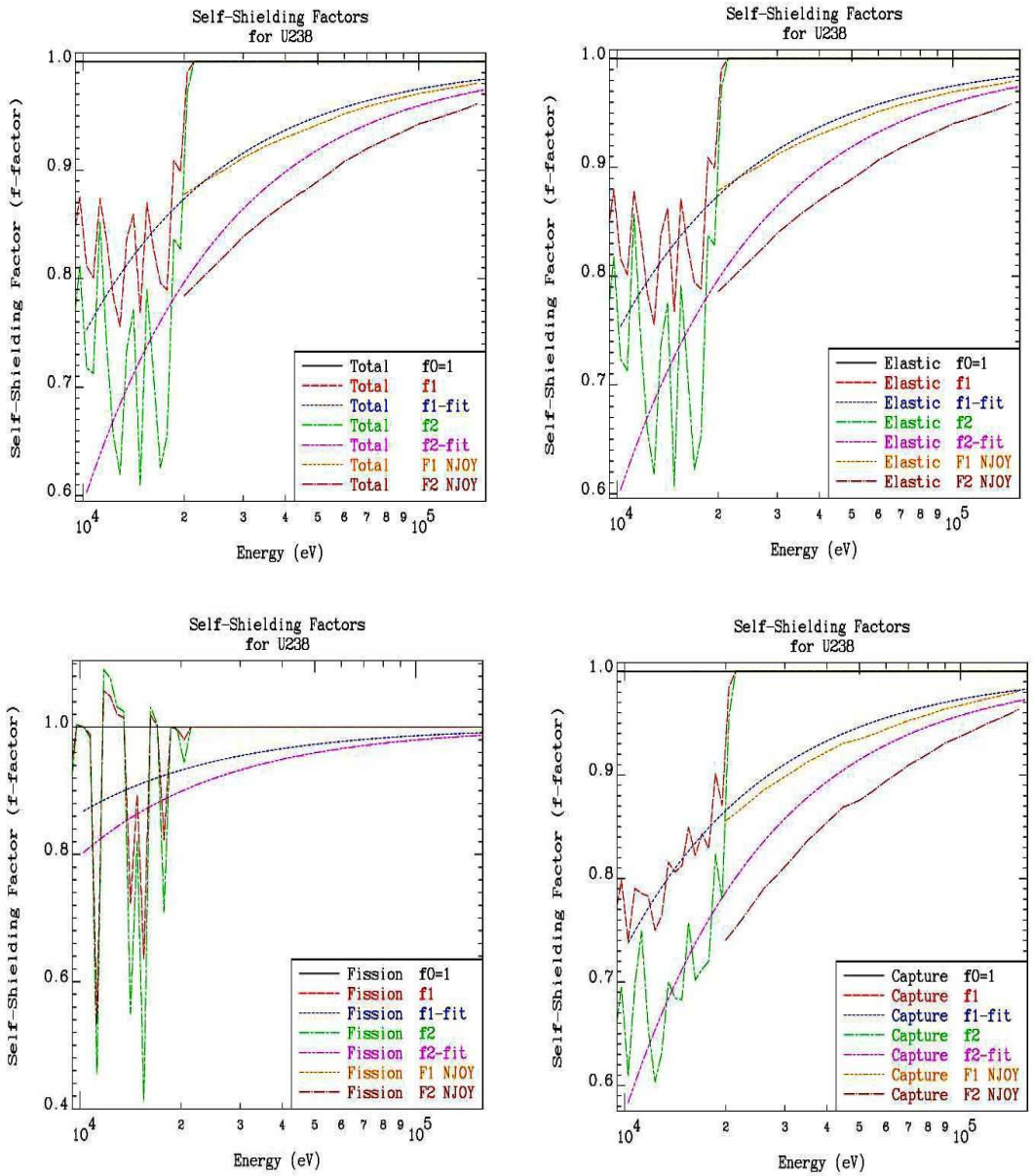

Fig. 6: *Self-shielding factors F_1 and F_2 for ^{238}U calculated by extrapolation and from the cross sections calculated by NJOY.*

^{239}Pu Comparison of Unresolved Resonance Region Self-Shielding Factors

The ^{239}Pu unresolved energy range is from 2.5 keV to 30 keV. Generally there is poor agreement between URRFIT and NJOY for both F_1 and F_2, with the NJOY data being generally lower than URRFIT; for Fission and Capture by NJOY the F_2 factors are even lower than the same factors over the entire resolved resonance range; physically there should be a smooth, continuous variation with energy from resolved to unresolved. URRFIT results show this, whereas NJOY results do not.

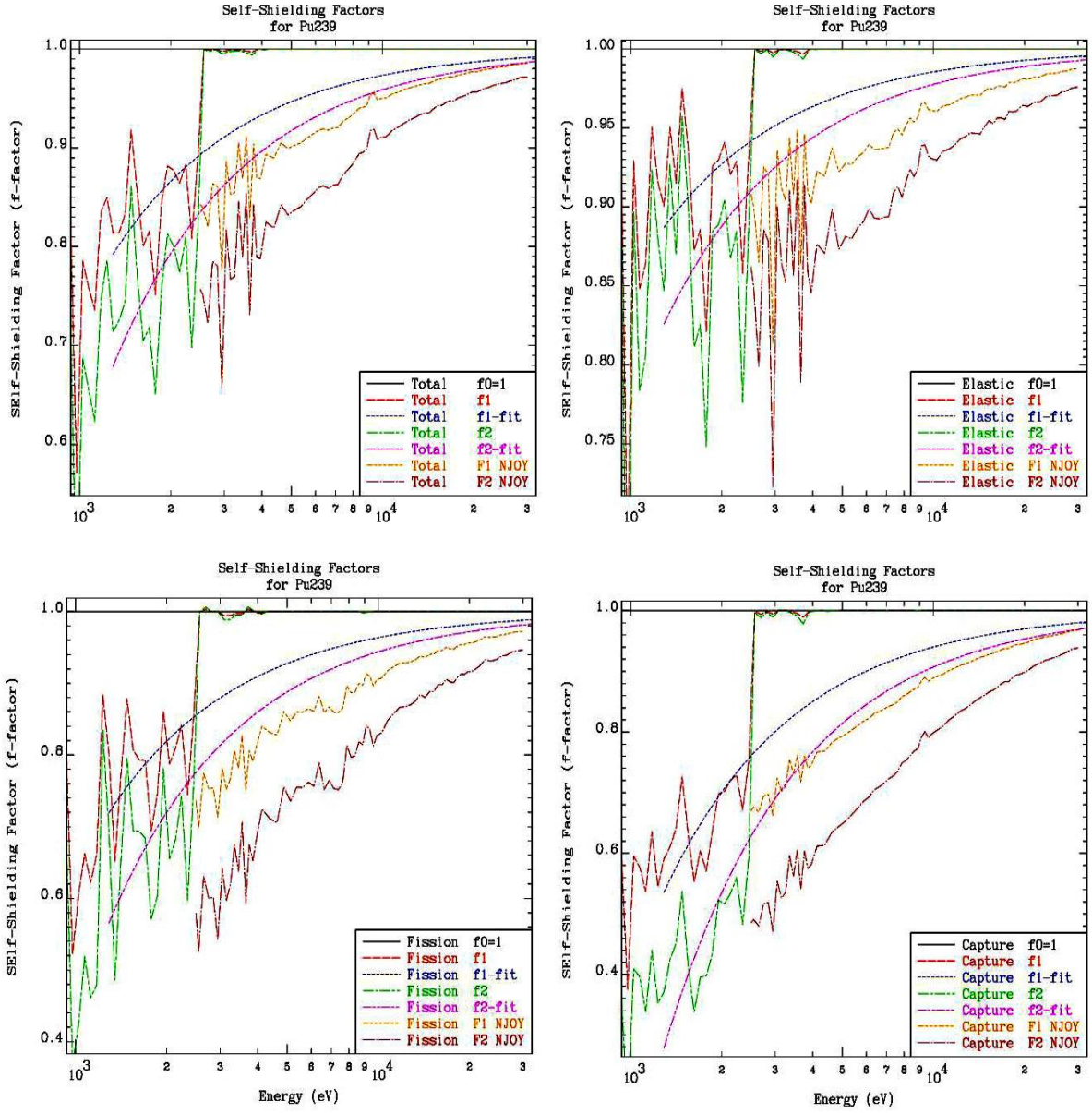

***Fig. 7**: Self-shielding factors F_1 and F_2 for ^{239}Pu calculated by extrapolation and from the cross sections calculated by NJOY.*

^{240}Pu Comparison of Unresolved Resonance Region Self-Shielding Factors

The ^{240}Pu unresolved energy range is from 5.7 keV to 40 keV. Generally there is poor agreement between URRFIT and NJOY for both Total and Elastic F_1 and F_2, with the NJOY data being generally lower than URRFIT. For Fission and Capture the results are in better agreement, particularly F_1 which is in very good agreement; physically there should be a smooth, continuous variation with energy from resolved to unresolved. URRFIT results show this, whereas NJOY results do not.

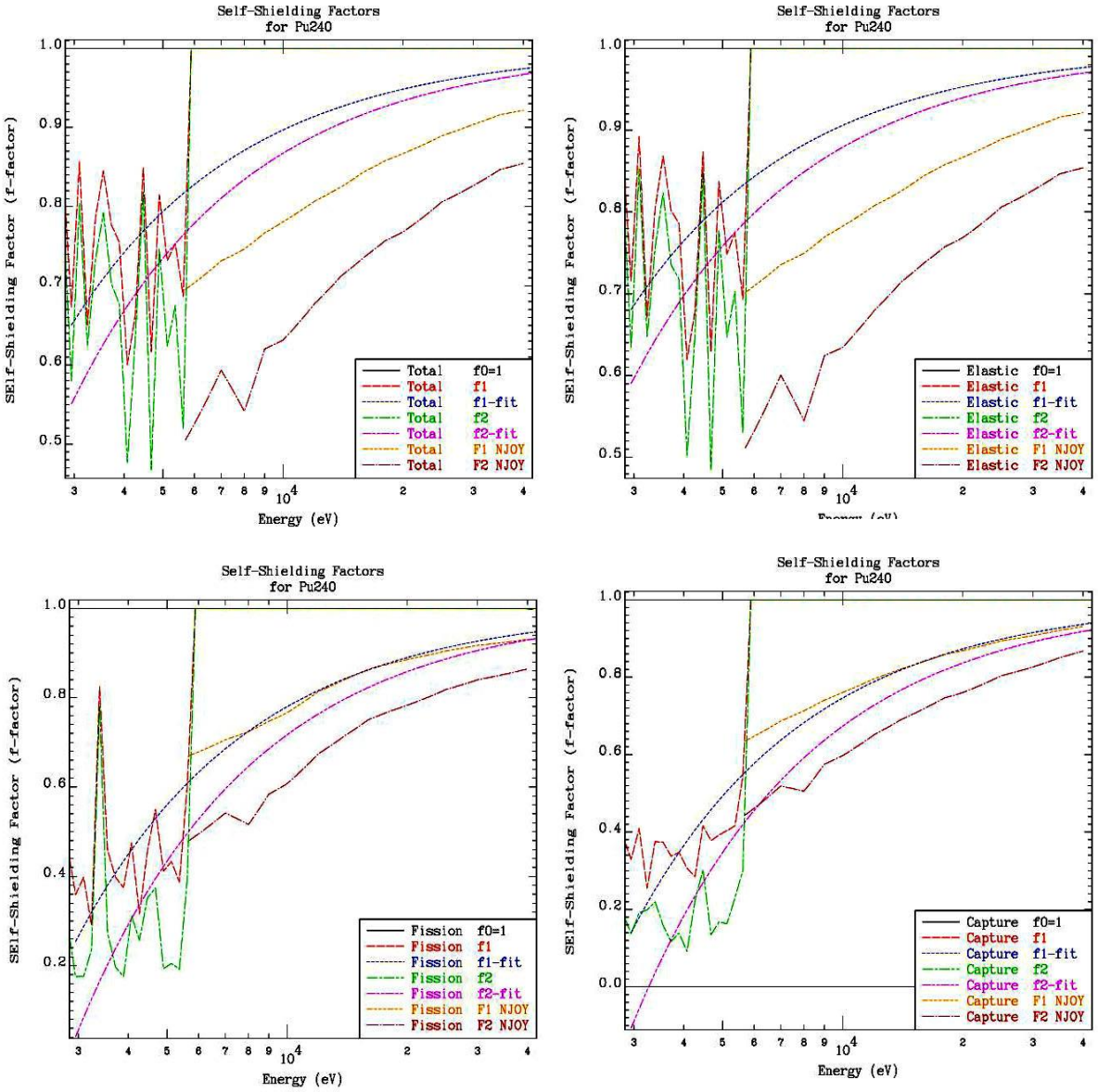

Fig 8: *Self-shielding factors F_1 and F_2 for ^{240}Pu calculated by extrapolation and from the cross sections calculated by NJOY.*

^{241}Pu Comparison of Unresolved Resonance Region Self-Shielding Factors

The ^{241}Pu unresolved energy range is from 300 eV to 40.2 keV. It is worth noting that today starting the unresolved region at such a low energy (300 eV) is very unusual, which at least partially explains the differences we see. Generally there is poor agreement between all of the URRFIT and NJOY data, with the NJOY data being generally lower than URRFIT. For Fission and Capture the NJOY F_2 factor is lower than the same factor over the entire resolved resonance range; physically there should be a smooth, continuous variation with energy from resolved to unresolved. URRFIT results show this, whereas NJOY results do not.

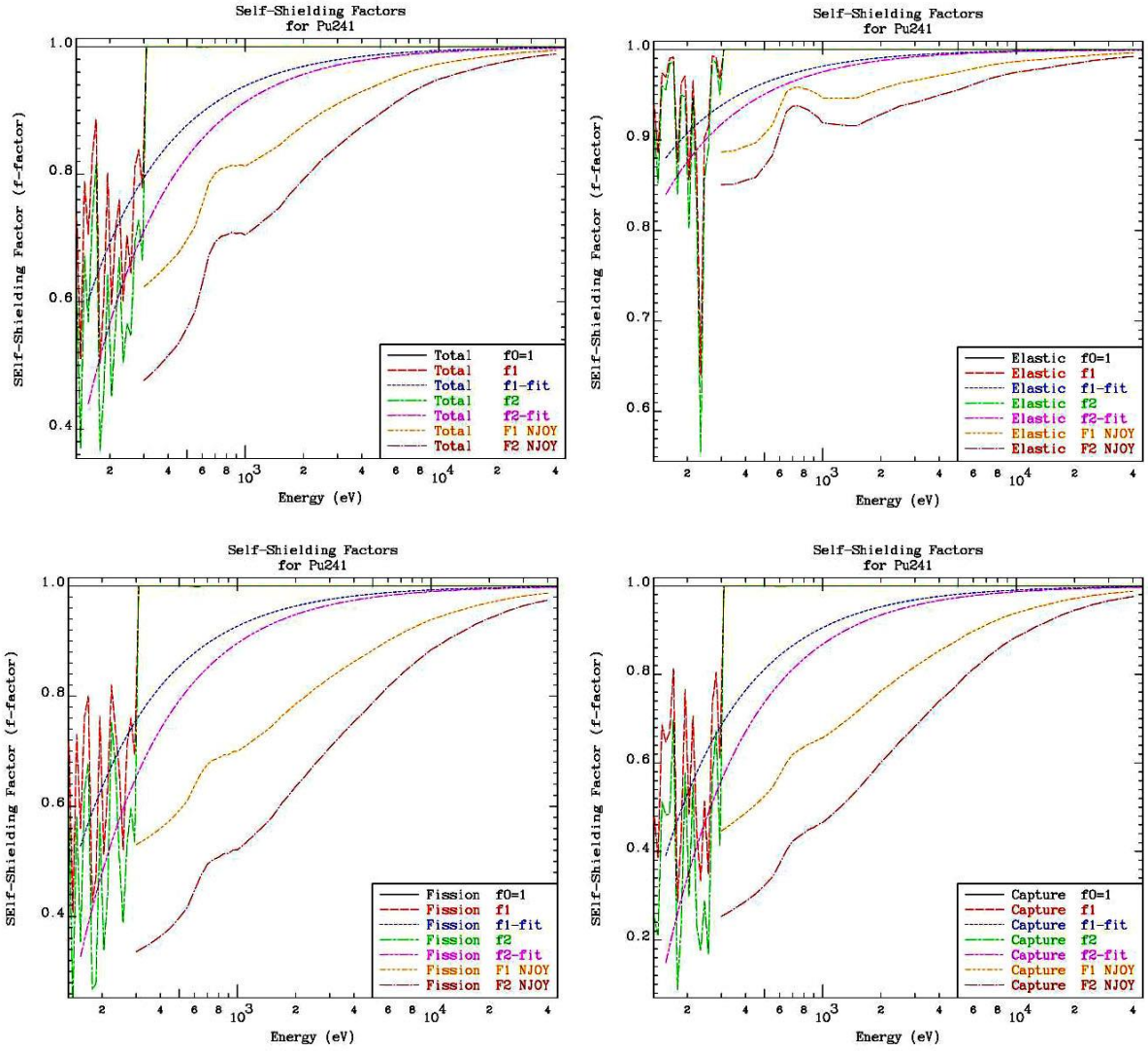

Fig. 9: *Self-shielding factors F_1 and F_2 for ^{241}Pu calculated by extrapolation and from the cross sections calculated by NJOY.*

Summary of Comparison of Unresolved Resonance Region Self-Shielding Factors

Based on the above comparison for five materials we can see the difficulty of trying to extrapolate the resonance self-shielding properties of a material using the ENDF convention of using average level spacing and widths for single level Breit-Wigner resonances and sampling ladders of resonances that have been Doppler broadened using a very approximate method of Doppler broadening, i.e. the so-called *psi-chi* method. Many years ago the author D.E. Cullen contacted Eugene Wigner [12], as an expert on Breit-Wigner resonances. He confirmed that the Breit-Wigner resonance formalism is designed to predict reaction rates near the peaks of resonances, but it is much less accurate in the minima between resonances. When in addition the psi-chi Doppler broadening method is used, the results between resonances are even worse - much worse. We must also add to this the uncertainty due to sampling ladders of resonances. In this situation we should not be surprised to find inconsistent results between what we calculate in the resolved and the unresolved energy ranges.

In comparison, extrapolating self-shielding properties from the resolved to unresolved energy ranges using moments of the cross section is relatively simple, straightforward and leads to consistent results, and avoid all of the restrictions involved with ENDF single level Breit-Wigner resonances, psi-chi Doppler broadening, and ladder sampling in the unresolved resonance energy region.

In summary, physically there should be a smooth, continuous variation with energy from the resolved to unresolved energy range. URRFIT results show this smooth, continuous results, whereas NJOY results do not. There seems to be little question that the approach presented here, to extrapolate moments, is physically more acceptable. Finally there is the investment of many hours of computer time to sample ladders – for each and every material – versus milli-seconds to extrapolate moments and define two band parameters from these moments.

How do these differences affect our K-eff results?

The below figure shows the results, including those based on URRFIT. As a reminder, the NJOY-PTM and URRFIT-MB results are completely independent being defined using two completely different methods. To be fair to both methods here we will not claim that one method is more or less accurate than the other, and as such in defining the ratios that appear on the below figure, the average of NJOY-PTM and URRFIT-MB results was used as the reference.

The results are not always as close as we found for the above figure, where the MCNP-PTM and MCNP-MB results were completely correlated, resulting in differences in the 0.01 to 0.02% range. But here we do find that the MCNP-PTM and URRFIT-MB results are still within a narrow range, +/- 0.1%, which is a realistically acceptable range; based solely on these results it would be hard to claim that one method is better or worse than the other for use in our applications. But based on the above comparison of resolved and unresolved data, it seems clear that extrapolating moments as has been done with TART for decades yields more physically acceptable results than the PTM approach, which is limited by single-level Breit-Wigner, very approximate Doppler broadening, and statistical variation due to sampling ladders.

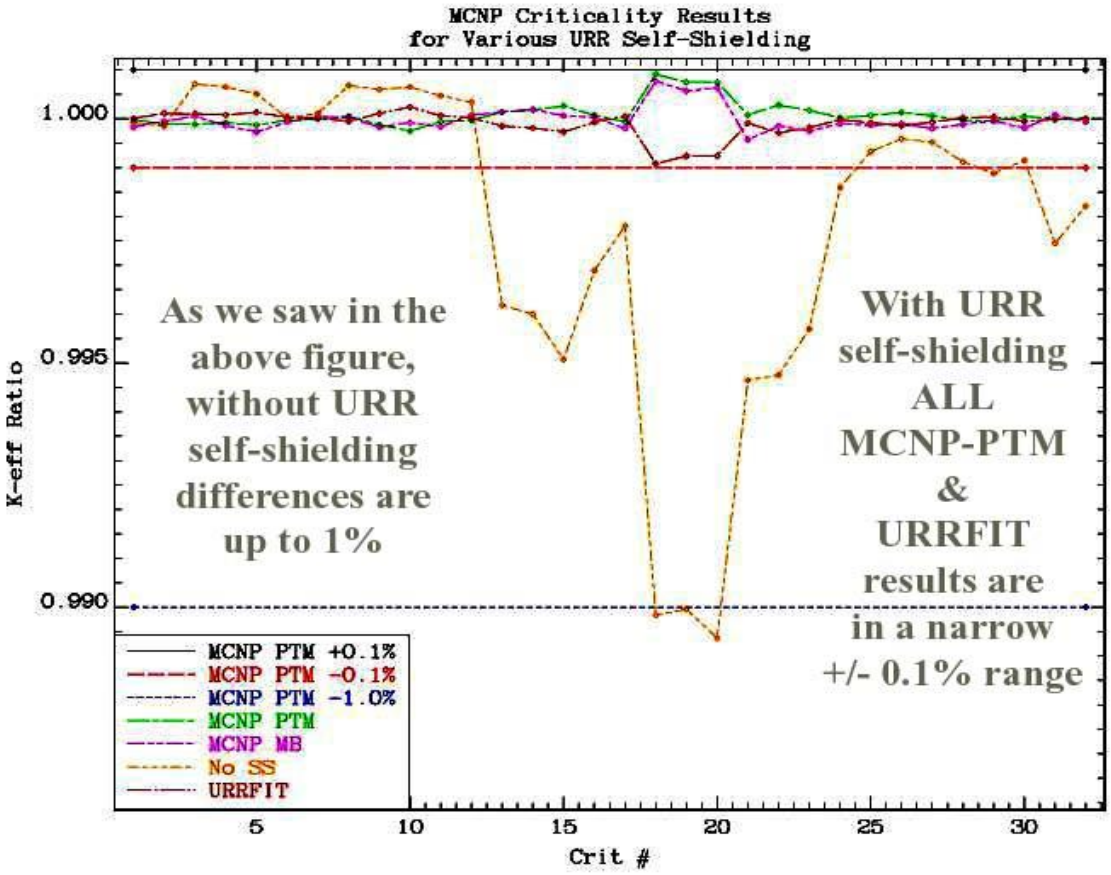

Fig. 10: *Comparison of K-eff values calculated using PTM and MB parameters.*

Appendix: 2 vs. 20 bands

The question that is most often asked when I describe the Multi-band (MB) method is: How can only 2 MB bands produce results that are as accurate as 20 PTM bands? The secret is in how the weights and cross sections for each band are defined. When Leo Levitt first introduced his Probability Table Method (PTM) it used only a few cross section ranges; back then PTM used ranges, in contrast today it uses discrete value, exactly the same as the multi-band method. Since then users have tried to improve results by adding more and more cross section bands, to the point where today NJOY/MCNP uses 20 bands.

It seems this was completely the wrong approach to take. Rather than more and more bands, what was needed was better physics to define the discrete quadrature used today by both PTM and MB; that's what it is: a discrete quadrature similar to the Gaussian quadrature used in the discrete-ordinates (Sn) codes, to approximate the angular distribution of neutrons or photons. What makes Gaussian quadrature so effective is how the weights and discrete directions are defined.

Similarly here we should examine more closely the approximations we are using to define the multi-band parameters (weights and discrete cross sections). As stated earlier, both PTM and MB are using a discrete quadrature to approximate the self-shielded cross section, or self-shielding factors,

$$<\sum_R (\Sigma_0)> = \frac{\sum_B \Sigma_{RB} P_B /[\Sigma_{tB} + \Sigma_0]}{\sum_B P_B /[\Sigma_{tB} + \Sigma_0]}$$

This includes the Bonderenko approximation that defines the self-shielded cross section as a continuous function of Σ_0 from 0 to infinity, as a sum of *B* bands. If one multiplies the numerator and denominator by the product of *B* terms he finds that we are actually defining the self-shielded cross section as a ratio of two (*B*-1) order polynomials in Σ_0 , which is a Pade approximation; (*B*-1) order polynomial includes *B* coefficients, starting with 0-th order up to (*B*-1)-th order.

What this means is that the PTM method in using 20 bands to represent this self-shielding curve; it is using polynomial in Σ_0 , up to 19-th order, whereas the MB method using only 2 bands is using only first order polynomials in numerator and denominator. The trick is that the multi-band method exactly conserves the self-shielded cross sections at the Σ_0 limits of 0 and infinity, whereas PTM do not explicitly conserve anything. The question is: Do we see any significant differences in the self-shielded curves based on 20 vs. 2 bands that will affect our integral results? Above in this report are results for the unresolved resonance ranges of some important nuclides that show no significant differences for an integral parameter such as K-eff..

To more clearly understand why we see so little difference between using 20 versus 2 cross sections bands we can look at how the self-shielding f-factors vary across the entire range of Σ_0 from small to large (basically Σ_0 zero to infinity). According to the approximations in our models this would include all possible combinations of one material and any other materials, e.g., ^{235}U mixed with anything else. Here we will scale everything to the infinitely

dilute total cross section, $<\sum_T(\infty)>$. The definition of the f-factors for the Total $F_1(T)$ and $F_2(T)$ is then,

$F_1(T) = \dfrac{\sum_B S_B P_B /[S_B + T]}{\sum_B P_B /[S_B + T]}$: sum over bands, B	$T = \sum_0 / <\sum_T(\infty)>$ $S_B = \sum_{TB} / <\sum_T(\infty)>$
$F_2(T) = \dfrac{\sum_B S_B P_B /[S_B + T]^2}{\sum_B P_B /[S_B + T]^2}$:sum over bands, B	$F_1(0)$ and $F_2(0)$ are the moments that are Extrapolated from Resolved to Unresolved

With this definition $F_1(T)$ approaches its maximum of 1.0 as $\sum_0$, or T approaches infinity (the infinitely dilute value) and its minimum as $\sum_0$, or T approaches zero (the totally shielded value, or reciprocal of the distance to collision).

Our two models differ only in how many bands are used: PTM uses 20 bands, and MB uses 2 bands, and how we define band weights and cross sections. You might think that the differences using 20 versus 2 would have to be very large in order to justifying requiring ten times as many bands. Let's see how the results actually compare at the lower and upper energy limits of a few unresolved resonance regions; we expect the maximum self-shielding near the lower energy limit and minimum near the upper energy limit. In all cases the self-shielding curve is a fairly simple S shape, as we see below.

For ^{235}U we see differences up to 0.017% at the lower energy limit (2.25 keV) and up to 0.001% at the upper energy limit (25 keV); the results are essentially indistinguishable.

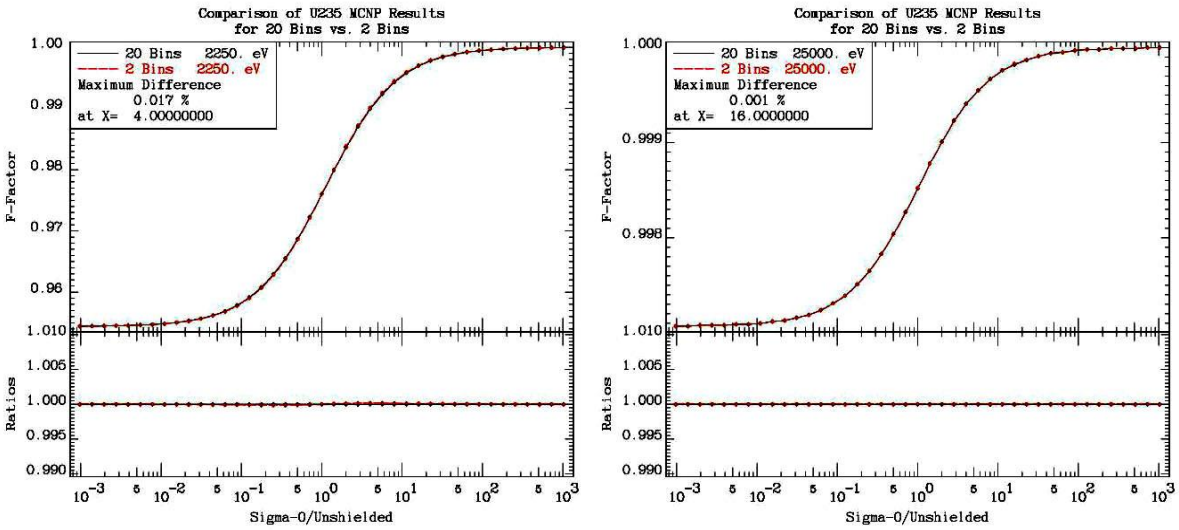

For ^{238}U we see differences up to 0.328% at the lower energy limit (20 keV) and up to 0.005% at the upper energy limit (near 149 keV); there is a small difference at 20 keV and virtually none at 149 keV. There is little significant difference that affects integral results (which help to explain why we saw no significant difference above for the K-eff values).

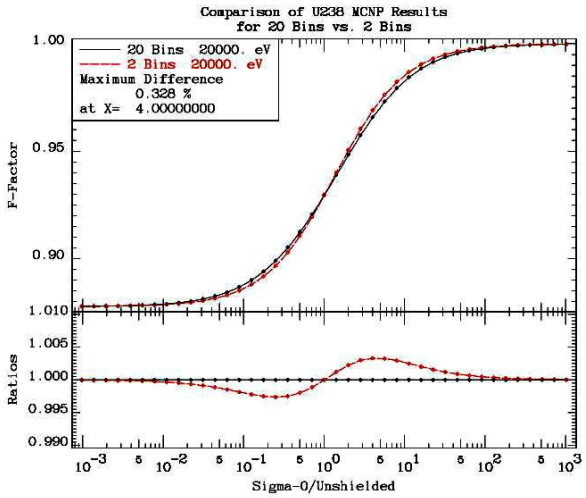

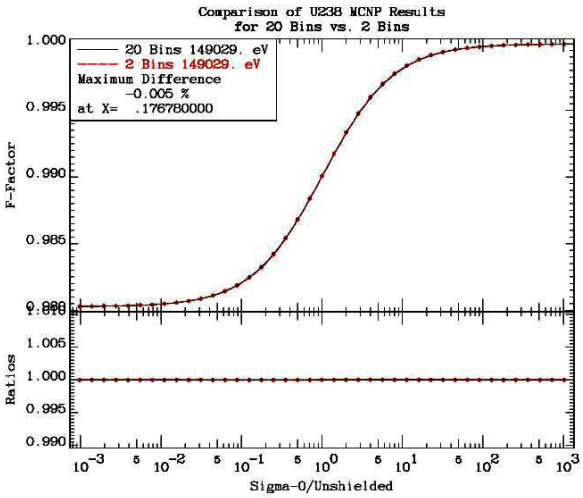

For ^{239}Pu we see differences up to 0.282% at the lower energy limit (2.5 keV) and up to 0.002% at the upper energy limit (near 30 keV); there is a small difference at 2.5 keV and virtually none at 30 keV. There is little significant difference that affects integral results (which help to explain why we saw no significant difference above for the K-eff values).

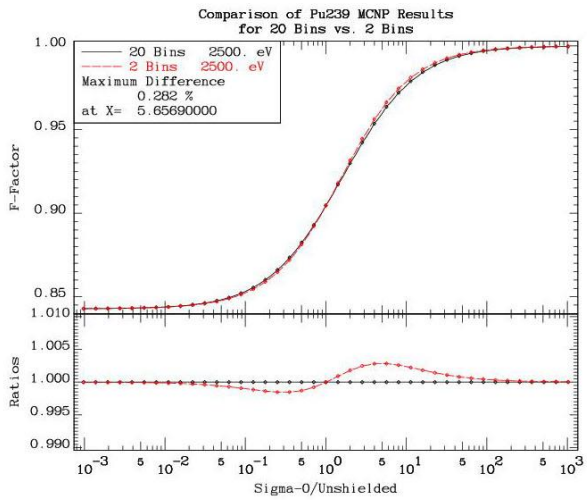

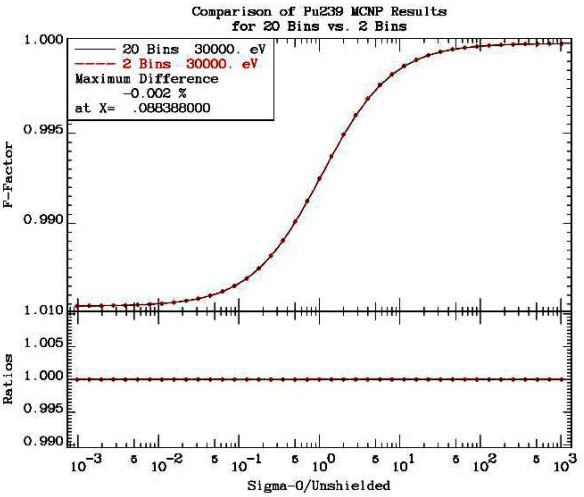

For ^{240}Pu we see differences up to 2.056% at the lower energy limit (5.7 keV) and up to 0.082% at the upper energy limit (near 40 keV); there is some difference at 5.7 keV and very little at 40 keV. Fortunately we would need an enormous concentration of ^{240}Pu to see any significant difference that affects integral results (which help to explain why we saw no significant difference above for the K-eff values).

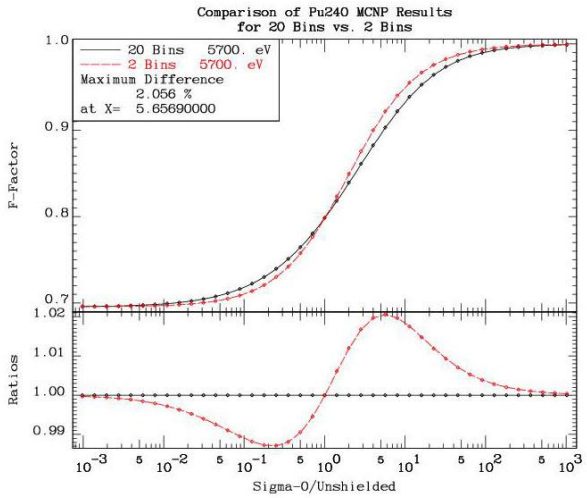

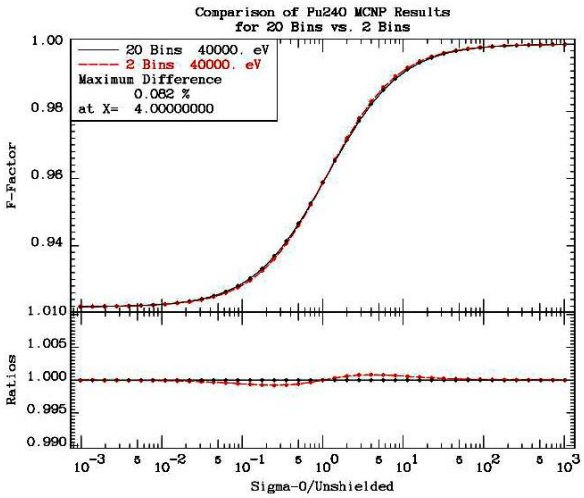

For ^{241}Pu we see differences up to 1.583% at the lower energy limit (300 eV) and up to 0.001% at the upper energy limit (near 40.2 keV); there is some difference at 300 eV and virtually none at 40.2 keV. The difference at 300 eV can be understood by noting how low in energy the resolved region ends and the unresolved starts, compared to other isotopes. Fortunately we would need an enormous concentration of ^{241}Pu to see significant difference that affects integral results (which once again explains why we saw no significant difference above for the K-eff values).

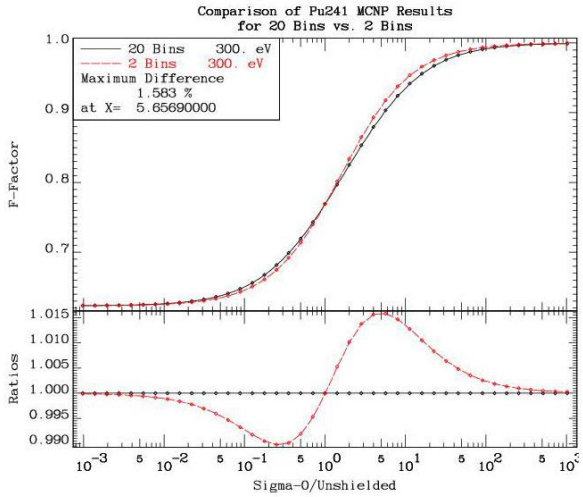

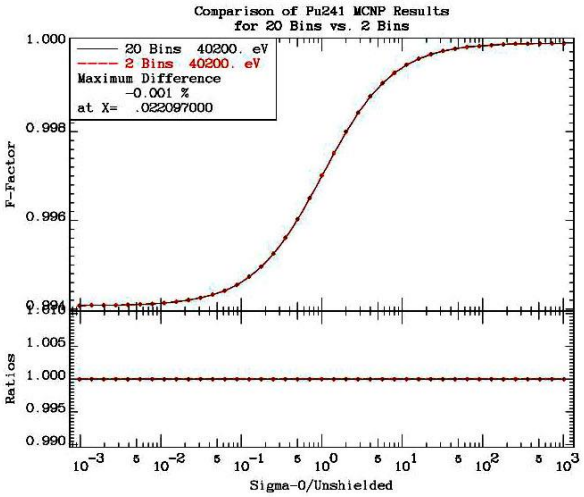

These results are quite typical and illustrate that in the unresolved resonance region the self-shielding curve is such a simple S shape that it does not require higher order polynomials in $\sum_0$ to accurately represent it. From the above figures we can see that the 2 bin MB results are defined to exactly agree with the 20 bin PTM results for the low and high limits of $\sum_0$ (at the extreme left and right of each figure), so that high and low concentrations of any material always produce the same results whether we use 20 or 2 bins.

In the above figures we only see differences, and even then only % differences, when the cross section due to one material is similar in magnitude to the cross section due to all other materials in a mixture. i.e., near the middle of each figure, where sigma-0/unshielded is close to 1. This rarely occurs in actual assemblies, and so far we are yet to encounter any critical assemblies where this is true, which helps to explains why the K-eff results we calculate is essentially the same whether we use 20 or 2 bins.

Please remember that the results of two sets of data, 20 bands vs. 2 bands, shown in the above figures, are exactly the two sets of data we used in our criticality calculations. In these criticality calculations for 32 critical assemblies we found that the difference in K-eff was usually less than 0.01% and always less than 0.02%, well below the 0.1% range that we consider of any significance. So that **the differences shown in the middle of self-shielding curves do not translate into any significant macroscopic differences, as in K-eff; the results are actually based on the lower and upper extremes of each self-shielding curve, where by definition the 20 band PTM and 2 band MB results agree.**

One important point to keep in mind is that this whole concept of the self-shielding curve vs. sigma-0 is based on some very approximate methods and assumptions, including: infinite media, narrow resonances, single level Breit-Wigner resonances, simplified Doppler broadening (such as psi-chi), and the Bonderenko approximation. In any real situation we do not expect the self-shielding to exactly agree with all of these approximations. In practice a good point to keep in mind is: **THAT WE DO NOT NEED AN EXACT ANSWER TO A VERY APPROXIMATE METHOD**. This statement may seem obvious to you, but what it means here is that in practice it is sufficient to conserve the unshielded and totally shielded limits for the scalar flux and partially shielded, which is what the multi-band method does, without necessarily agreeing with the entire VERY THERETICAL self-shielding curve.

Generally the self-shielding of heavy even-odd isotopes, such as ^{235}U, ^{239}Pu and ^{241}Pu, is small compared to that of even-even isotopes ^{238}U and ^{240}Pu, e.g., note the value of f-factor near the lower sigma-0 limit of the above figures. This makes it easier to represent the self-shielding of these even-odd isotopes, i.e., our important fuels.

In summary, as with any discrete quadrature, such as Gaussian quadrature, or as in our case multi-band quadrature, what is most important is how the discrete weights and ordinates are defined. For Gaussian quadrature the weights and ordinates are defined to approximate polynomials, e.g., *N*-th order Gaussian quadrature has 2**N* degrees of freedom (N weights and N ordinates), so that it can exactly represent any 2**N* order polynomial.

To illustrate a similarity to our situation, consider that we want to define the integral of a function(x). You can try to accurately integrate a curve by using equally or regularly spaced intervals in x, and can use a brute force approach of using more and more values of x to try

and improve your integral. Alternatively, you can use a Gaussian quadrature, to guarantee that you will get the best answer for any polynomial of order 2*N.

This is quite similar to our situation where starting from Leo Levitt's original Probability Table Method (PTM) using a few cross section bands, over the years users have tried the brute force approach to using more and more bands. In contrast I have tried to use a more scientific approach to concentrate on defining the multi-band weights and ordinates to accurately estimate the actual, real scalar moments of the flux that we encounter in our applications.

Analytical Solution for Band Parameters

The much of following section is copied from Handbooks, Ref. [6] and [7], which the author D.E. Cullen wrote as long ago as 1987, so this is nothing new. I have included changes here to both correct typos in Ref. [6] and [7], and updates to the procedures I now use to define multi-band parameters.

The equations defining the multi-band parameters are non-linear and have a non-unique solution, e.g., we can interchange the multiple solutions to define another solution. This has resulted in people trying iterative solutions, which are difficult, and numerically unstable. This is not necessary: you know how to solve non-linear, non-unique equations; you were taught as a teenager how to solve a quadratic $a*X^2 + b*X + c = 0$, by assuming X = A+/-B.

$$X = \{-b +/- [b^2 - 4*a*c]^{1/2}\}/\{2*a\} \quad : A = -b/\{2a\} \quad : B = [b^2 - 4*a*c]^{1/2}/\{2*a\}$$

The two band equations are no more complicated than this. The two band equations are just quadratic. Similarly the three band equations are cubic and the four band quartic; all of these have simple analytical solutions based on nothing more complicated than a change of variables. Here we illustrate the simple analytical two band solution (the following is mostly copied from Ref. [6], [7], with corrections to typos in Ref. [6], [7], and updated for the method I use today).

Since we know the forms that we expect the self-shielded moments of the flux to assume in a number of widely applicable cases, we will define our quadrature to ensure that in these cases we obtain exactly the correct self-shielded cross sections. For example, if we have a standard self-shielded multigroup library for each group, material and reaction, we will have a variety of self-shielded cross sections, each corresponding to using a different self-shielding factor in the form (I define these using my GROUPIE code, which is part of PREPRO2015 [10]),

$$W(\Sigma_T) = \frac{1}{[\Sigma_T + \Sigma_0]^k} \text{ ; for various } k \text{ and } \Sigma_0$$

Since from this library we know the self-shielded cross section corresponding to each self-shielding factor (the equivalent of $W(\Sigma_T)$), we can use this information to solve the system of equations to define our multi-band weights, P_B, and cross sections, Σ_{RB}, for each band.

Analytical Solution for 2 Bands

In order to illustrate how to define multi-band parameters, consider the simplest possible case of using two bands; in this case we have four unknowns, the two band weights P_1 and P_2, and the two band cross sections Σ_{R1} and Σ_{R2}, for each reaction R (R = total, elastic, capture,...). In order to uniquely define our four unknowns for the total cross section we need four equations. One of the four equation normalizes our quadrature $P_1 + P_2 = 1$. In addition to will use three moments of the total cross section to complete our set of four equations.

As with any quadrature, such as Legendre, we can define our quadrature in more than one way to best meet our needs. In each case I use moments of the cross section to define quadrature ordinates and abscissa. In both cases I want to be sure to exactly reproduce the results for certain limiting cases that we may actually encounter in our applications; these include the infinitely dilute, or unshielded limit ($W(\Sigma_T)=1$), the totally shielded flux weighted cross section ($W(\Sigma_T)=1/\Sigma_T$), or distance to collision. To uniquely define the quadrature I need three moments.

The first method that I used many years ago, and documented in ref. [6] and [7], used the totally shielded current weighted cross section ($W(\Sigma_T)=1/\Sigma_T^2$). The second method, that I have used more recently, uses a partially shielded weighted cross section, with a value of Σ_0 equal to the unshielded total cross section in each group ($W(\Sigma_T)=1/(\Sigma_T+\Sigma_0)$. Many years of experience have shown that the second method yields better results (i.e., better agreement with continuous energy cross section calculations), so that today this is what I personally use as my standard in all of my calculations [9]. The first method that I initially used many years ago is described in detail in ref. [6] and [7], and I will not describe further here; here I will only describe the second method, because this is what I use today.

In order to illustrate this procedure, consider the simplest possible case of using two bands; in this case for the we have four unknowns, the two band weights P_1 and P_2, and the two band cross sections Σ_{R1} and Σ_{R2}, for each reaction R (R = total, elastic, capture,...). Assume that from a normal multigroup processing code we have calculated the unshielded cross section ($W(\Sigma_T)=1$), the totally shielded flux weighted cross section ($W(\Sigma_T)=1/\Sigma_T$) and the partially shielded flux weighted cross section ($W(\Sigma_T)=1/(\Sigma_T + <\Sigma_0>)$), which we will denote by $<\Sigma_0>,<\Sigma_1>,<\Sigma_2>$, respectively. Then for the total cross section ($\Sigma_R=\Sigma_T$), the four equations sufficient to uniquely calculate our two band parameters are obtained by realizing that our quadrature must be normalized,

$$P_1 + P_2 = 1$$

and by inserting each our three weighting functions into our equation and equating the resulting equations to our known, three pre-calculated self-shielded cross sections, $<\Sigma_0>,<\Sigma_1>,<\Sigma_2>$,

$$<\Sigma_0> = \frac{\Sigma_{T1}P_1+\Sigma_{T2}P_2}{P_1+P_2} \quad ; \quad (W(\Sigma_T)=1)$$

$$<\Sigma_1> = \frac{P_1 + P_2}{P_1 X_{T1} + P_2 X_{T2}} \quad ; \quad (W(\Sigma_T) = X_T) : \; X_T = 1/\Sigma_T$$

$$<\Sigma_2> = \frac{P_1 \Sigma_{T1} X^*_{T1} + P_2 \Sigma_{T2} X^*_{T2}}{P_1 X^*_{T1} + P_2 X^*_{T2}} \quad : \quad (W(\Sigma_T) = X^*_T) \; : X^*_T = 1/[\Sigma_T + <\Sigma_0>]$$

We obtain a set of four nonlinear equations in four unknowns. Unfortunately, the solution to this set of equations is not unique. For example, the two bands are indistinguishable, so that if we obtain one solution for this system of equations, we can obtain a second solution merely by exchanging the weights and cross sections for the two bands. The solution does not become unique until we introduce an ordering into the parameters, such as $\Sigma_{T1} \leq \Sigma_{T2}$. This leads us to believe that the two band parameters will be related to the roots of a quadratic equation, which are also not unique without an ordering. Therefore, we make the standard change of variables used to solve a quadratic equation,

$$P_1 = \frac{1}{2} + \delta \quad ; \Sigma_{T1} = \frac{1}{X_1} = \frac{1}{A + B}$$

$$P_2 = \frac{1}{2} - \delta \quad ; \Sigma_{T2} = \frac{1}{X_2} = \frac{1}{A - B}$$

This change of variables immediately satisfies $P_1 + P_2 = 1$ and the remaining three equations can be analytically solved to define,

$$A = \frac{1}{2 <\Sigma_1>} \left[\frac{<\Sigma_0> - <\Sigma_1>}{<\Sigma_0> - <\Sigma_2>} \right]$$

$$B^2 = \{ <\Sigma_1> A \, [<\Sigma_0> A - 2] + 1 \} / [<\Sigma_0><\Sigma_1>]$$

$$\delta = \frac{1 - A <\Sigma_1>}{2B <\Sigma_1>}$$

WARNING – the above definition of B^2 is correct; there was a typo in all earlier versions of the documentation, including the original version of this report and ref. [6] and [7]. This only effects the documentation; the codes GROUPIE [10], URRDO and URRFIT have always used the correct definition of B^2.

As expected there are two possible values for B, corresponding to the positive and negative roots of B^2. This is the result of the non-uniqueness of the solution without an ordering. From the definitions of Σ_{T1}, Σ_{T2} and δ in terms of A and B, equation [4.236] we can see that choosing the positive or negative root of B^2 merely corresponds to the same solution with the two bands interchanged. In order to obtain a unique solution we will always define B to be positive, which corresponds to introducing the ordering $\Sigma_{T1} \leq \Sigma_{T2}$.

The above algorithm will always produce physically acceptable parameters (positive band weights and cross sections) as long as $<\Sigma_0> \geq <\Sigma_1> \geq <\Sigma_2>$. It can be demonstrated

(see Ref. [6], [7]), that the only time that the three of these are equal is when the total cross section is independent of energy across the group (i.e., when it is constant); in all other cases this inequality is true. When the cross section is constant the two bands become indistinguishable and the two band cross sections become equal, i.e., only one band is required in the group (i.e., the normal multigroup equation) – WARNING – this is a limiting case that the codes URRDO and URRFIT explicitly handle to avoid a singularity in the above definitions, as B and δ approach zero; this limit and how I handle it is described below.

Once the two band parameters for the total cross section are known, for each other reaction R (R = elastic, capture, fission, etc.), we may solve for the reaction cross sections. For this two band example for each reaction there will be two unknowns, the two band cross sections Σ_{R1} and Σ_{R2}. If from our normal multigroup library for each reaction we know the unshielded cross section $(W(\Sigma_T)=1)$ and the totally shielded flux weighted cross section $(W(\Sigma_T)=1/\Sigma_T)$, we will have two equations for each reaction R,

$$<\Sigma_0>_R = \frac{\Sigma_{R1}P_1+\Sigma_{R2}P_2}{P_1+P_2} \quad ; \ (W(\Sigma_T)=1)$$

$$<\Sigma_1>_R = \frac{\frac{\Sigma_{R1}P_1}{\Sigma_{T1}}+\frac{\Sigma_{R2}P_2}{\Sigma_{T2}}}{\frac{P_1}{\Sigma_{T1}}+\frac{P_2}{\Sigma_{T2}}} \quad ; \ (W(\Sigma_T)=1/\Sigma_T)$$

Since from the total cross section definitions, we know P_1 , P_2, Σ_{T1} and Σ_{T2}, we may solve these two **linear** equations to define the unknowns Σ_{R1} and Σ_{R2}. In order to solve these two equations, it is convenient to introduce the change of variables,

$$\Sigma_{R1} = <\Sigma_0>_R - \frac{C}{P_1}$$

$$\Sigma_{R2} = <\Sigma_0>_R + \frac{C}{P_2}$$

This change of variables immediately satisfies the first equation, and the second can be solved to find,

$$C = [<\Sigma_0>_R - <\Sigma_1>_R][\frac{\frac{P_1}{\Sigma_{T1}}+\frac{P_2}{\Sigma_{T2}}}{\frac{1}{\Sigma_{T1}}-\frac{1}{\Sigma_{T2}}}] = [<\Sigma_0>_R - <\Sigma_1>_R]/[2B<\Sigma_1>_T]$$

In the seemingly trivial limit of no self-shielding, these equations become numerically unstable, because in this limit and two band cross sections, Σ_{T1} and Σ_{T2}, approach the unshielded average, and the two band weights, P_1 and P_1 , become non-unique, as long as they sum to unity, e.g., we can see this from the equations defining B and δ , since in the no shielding limit B approaches zero and since δ is proportional to $1/B$, we have a problem.

To handle this limit I consider three cases. In all three cases I always define,

$$P_1 = \frac{1}{2} + \delta \quad ; \Sigma_{T1} = \frac{1}{X_1} = \frac{1}{A+B}$$

$$P_2 = \frac{1}{2} - \delta \quad ; \Sigma_{T2} = \frac{1}{X_2} = \frac{1}{A-B}$$

The three cases correspond to placing limits on δ and/or B .

1) **No self-shielding**: $<\Sigma_1> = <\Sigma_0>$

Weight	$W(\Sigma_T)=1$
Conserve	$<\Sigma_0>$

P1 = P2 = 1/2 : $\delta = 0,\ B^2 = 0,\ A = 1/<\Sigma_0>$

$\Sigma_{T1} = \Sigma_{T2} = <\Sigma_0>$

2) **Little self-shielding**: $<\Sigma_1> \Rightarrow 0.9999 <\Sigma_0>$; 0.01% or less self-shielding

Weight	$W(\Sigma_T)=1$	$W(\Sigma_T)=1/\Sigma_T$
Conserve	$<\Sigma_0>$	$<\Sigma_1>$

P1 = P2 = 1/2 : $\delta = 0$

$A = 1/<\Sigma_1>$

$B^2 = [<\Sigma_0> - <\Sigma_1>]/[<\Sigma_0><\Sigma_1>^2]$

3) **General self-shielding**: $<\Sigma_1> < 0.9999 <\Sigma_0>$; more than 0.1% self-shielding

Weight	$W(\Sigma_T)=1$	$W(\Sigma_T)=1/\Sigma_T$	$W(\Sigma_T)=1/(\Sigma_T + <\Sigma_0>)$
Conserve	$<\Sigma_0>$	$<\Sigma_1>$	$<\Sigma_2>$

$$A = \frac{1}{2<\Sigma_1>}\left[\frac{<\Sigma_0> - <\Sigma_1>}{<\Sigma_0> - <\Sigma_2>}\right]$$

$$B^2 = \{<\Sigma_1> A\,[<\Sigma_0> A - 2] + 1\}/[<\Sigma_0><\Sigma_1>]$$

$$\delta = \frac{1 - A<\Sigma_1>}{2B<\Sigma_1>}$$

I repeat the WARNING – the above definition of B^2 is correct; there was a typo in all earlier versions of the documentation, including the original version of this report and ref. [6] and [7]. This only effects the documentation; the codes GROUPIE [10], URRDO and URRFIT have always used the correct definition of B^2.

From the above equations we can see that for any reaction where the unshielded and shielded cross sections $<\Sigma_0>_R$ and $<\Sigma_1>_R$ are equal, we find $C = 0$, and the two band cross sections will be the same in both bands and equal to their normal unshielded multigroup average. This will be the case for reactions that do not include resonant structure. Therefore normally in

using the multi-band method we calculate multi-band parameters for total, elastic, capture and fission, and to use the normal multigroup unshielded cross section for all other reactions. NJOY/MCNP attempt to account for self-shielding from other reactions (particularly inelastic) by defining "competition" as the total minus elastic, capture and fission.

WARNING: The codes URRDO and URRFIT both use a single subroutine to start from cross section model and define two band parameters. This subroutine handles all special cases, e.g., no self-shielding, little self-shielding, etc., and it is highly recommended that if you want to produce two band parameters that you use this subroutine.

Once these two band parameters have been defined, they may be used in transport calculations and they will correctly reproduce the limiting cases of unshielded and totally shielded flux. For example, again consider a piece of ^{232}Th in which we will use two band parameters to produce energy, spatially and directionally dependent self-shielding. In this case the combination of the two bands at the boundary (surface) for directions oriented into the ^{232}Th will combine to produce the correct equivalent of the unshielded group averaged cross section. However, deep within the ^{232}Th the flux in the band with the higher of the two band cross sections will be suppressed, relative to the other band, and the equivalent group averaged cross sections will approach their self-shielded value, i.e., we are reproducing continuously varying spatially dependent self-shielding. If we consider the albedo from the surface the flux in the higher cross section band will again be suppressed, relative to the other band, which will result in self-shielding, i.e., we are reproducing directionally dependent self-shielding, with the flux incident on the slab unshielded, and at exactly the same spatial point, the albedo from the slab is self-shielded.

Note the implications here: In principle, since self-shielding is directionally and spatially dependent an S_N code really should use differently shielded cross sections in each direction and in each spatial zone. In practice, all of these directional and spatial effects can be reproduced by using only 2 band cross sections, the same 2 band cross sections in all directions and over large spatial regions.

Generalization to N Bands

Today in the Unresolved Resonance Region we never need more than two cross section bands, but if you wish to use the multi-band method in general, over a more extended energy range, as for example in a deterministic multigroup code [5, 6, 7], you may want to consider an addition band.

The procedures introduced above to define two band parameters may be generalized to define the band parameters for any number of bands per group. In general the equations are a system of coupled, nonlinear algebraic equations. Given a set of self-shielded cross sections, this system must be solved for the band cross sections Σ_{RB} and Σ_{TB} and band weights P_B.

This is a classic moments' problem: for $\Sigma_0 = 0$ and various values of N, it is the Hausdorff moments problem, while for N = 1 and various values of Σ_0 it is the Stieltjes-Hilbert moments problem. Both of these problems have been widely studied, and only pertinent results will be given here.

First take R = total. In this case, for N bands we have 2N unknowns: they are P_B and Σ_{TB}, for B = 1,2,…,N. Given 2N values of the self-shielded total cross sections (defined for 2N different combinations of Σ_0 and N), the system of equations can be solved uniquely for P_B and Σ_{TB}. Given more than 2N values of the self-shielded cross section, the system can be solved in some "best fit" sense (e.g., least squares or min-max).

Once the P_B and Σ_{TB} are known, the system of equations is linear in the N unknowns Σ_{RB} for R = elastic, capture, fission; given N or more values of the self-shielded cross section for reaction R, the system is easy to solve uniquely or in some "best fit" sense.

Reality Check: How Accurately can we Really Calculate Critical Assemblies

Throughout this report we have repeatedly stated that today we like to assume (hope) that we can calculate critical assemblies – any assembly - to within about +/- 0.1%. The focus of this paper is not on the ability of our codes to reproduce measured results; it is on the very narrow subject of self-shielding in the unresolved resonance region, and how calculated results are effected by using one model vs. another, i.e., 20 PTM bands vs. 2 MB bands.

Still it is interesting to have a reality check and see how accurately we can really calculate critical assemblies. I (D.E. Cullen) did this sometime ago to test 1,172 critical assemblies [11], using the ENDF/B-VII data [1] and the TART Monte Carlo code [9]. That report shows the realistic range of results calculated, and in particular shows that while the average summed over many assemblies may be very close to 1.0, there is a fairly wide spread in individual results which is much larger than the +/- 0.1% we hope we can achieve.

Below are results for the 32 critical assemblies used in this study, and includes a comparison between Measured and MCNP Calculated results. In this case of the 32 cases, 10 are within +/- 0.1%, most are within 1.0%, and 3 are outside +/- 1.0%. I need not say more here than to merely state that this is reality, not the 0.1% widely claimed. PLEASE keep this in mind when judging Measured vs. Calculated results. It isn't enough to claim you used the latest ENDF/B library and a widely used and respected Monte Carlo code, such MCNP; much more

goes into achieving agreement, particularly with regard to the geometric model and material composition, which can greatly limit accuracy, and we the code developers and users have little control over the accuracy of published models [8]. So CAVEAT EMPTOR (let the user beware).

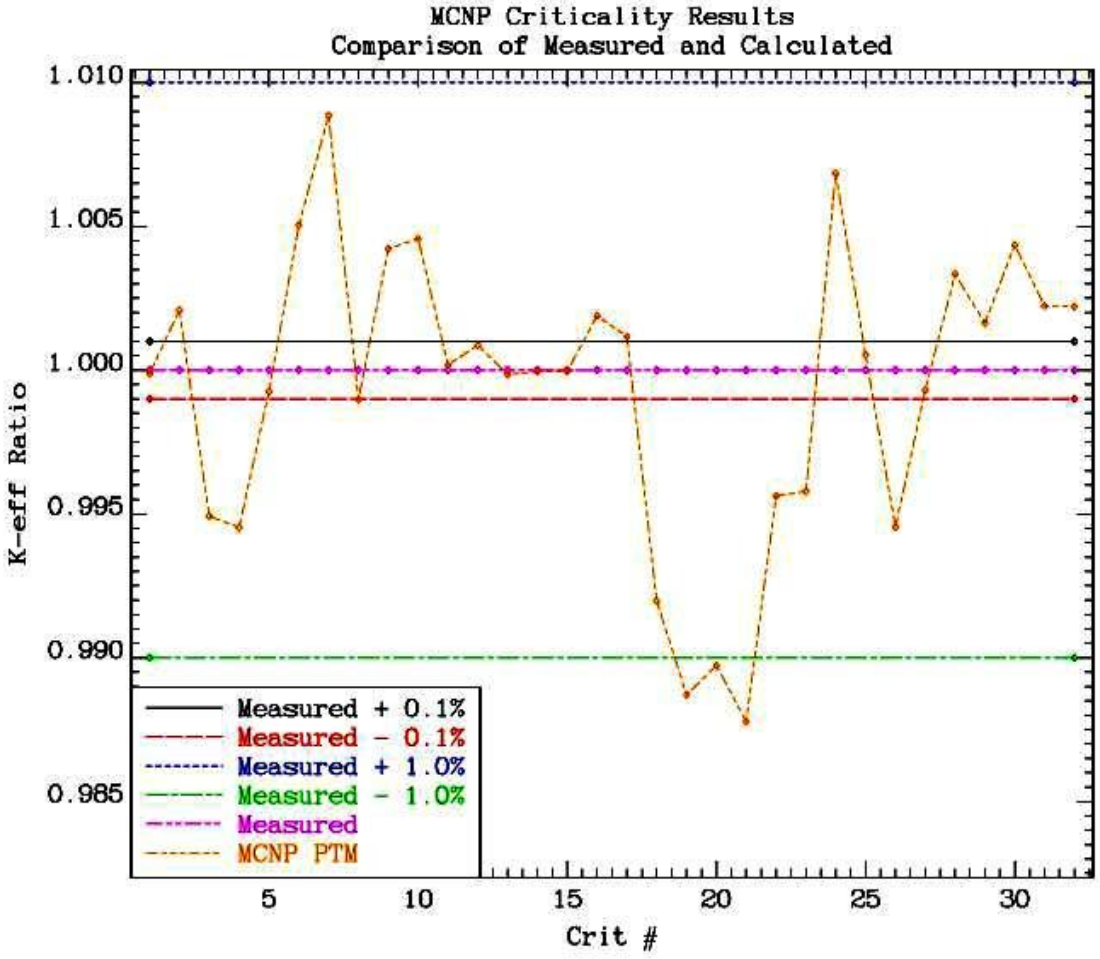

References

[1] ENDF-6 Formats Manual Data Formats and Procedures for the Evaluated Nuclear Data File ENDF/B-VI and ENDF/B-VII, Written by the Members of the Cross Sections Evaluation Working Group Last Revision Edited by M. Herman and A. Trkov, June 2009.

[2] R.E. MacFarlane, *et al*., The NJOY Nuclear Data Processing System, Version 2012, LA-UR-12-27079, August 2013.

[3] L.B. Levitt, The probability table method for treating unresolved resonances in Monte Carlo, BNL-50387 (ENDF-187), May 1972.

[4] MCNP - A General Monte Carlo N-Particle Transport Code, Version 5, Vol. I: Overview and Theory, X-5 Monte Carlo Team, Los Alamos National Laboratory report LA-UR-03-1987 (April 24, 2003).

[5] D.E. Cullen, Application of the probability table method in multi-group calculations, BNL-50387 (ENDF-187), May 1972.

[6] Nuclear Cross Section Processing (Yigal Ronen, Ed.), Handbook of Nuclear Reactor Calculation, Vol. I, CRC Press, inc., Boca Raton, Florida (1986).

[7] "Nuclear Data Preparation", in: The Handbook of Nuclear Engineering, Springer Publishing, NY, NY (2010), Vol. 1, pp. 279-425.

[8] International Criticality Safety Benchmark Evaluation Project (ICSBEP), NEA-1486/14, ICSBEP2015-Handbook, Nuclear Energy Agency (2015).

[9] D.E. Cullen, TART2012: An Overview of A Coupled Neutron-Photon, 3D, Combinatorial Geometry, Time Dependent Monte Carlo Transport Code, LLNL-TR-577352, June 2012.

[10] D.E. Cullen: PREPRO2015: 2015 ENDF/B Pre-processing Codes, IAEA-NDS-39, Rev. 16, January 2015.

[11] D.E. Cullen and E.F. Plechaty, ENDF/B-VII.0 Data Testing Using 1,172 Critical Assemblies, Lawrence Livermore National Laboratory, UCRL-TR-235178, October 2007

[12] Eugene Wigner, Private Communication, circa 1980.